AFM Investigations of Phase Separation in Supported Membranes of Binary Mixtures of POPC and an Eicosanyl−Based Bisphosphocholine Bolalipid

ARTICLE *in* LANGMUIR · JUNE 2010

Impact Factor: 4.46 · DOI: 10.1021/la904532s · Source: PubMed

5 AUTHORS, INCLUDING:

David Brownholland
Carthage College
3 PUBLICATIONS **11** CITATIONS
SEE PROFILE

David H Thompson
Purdue University
112 PUBLICATIONS **3,125** CITATIONS
SEE PROFILE

Published in final edited form as:
Langmuir. 2010 June 1; 26(11): 8525–8533. doi:10.1021/la904532s.

AFM Investigations of Phase Separation in Supported Membranes of Binary Mixtures of POPC and an Eicosanyl-based Bisphosphocholine Bolalipid

Kirk Mulligan[a], **David Brownholland**[b], **Anna Carnini**[a], **David H. Thompson**[b,*], and **Linda J. Johnston**[a,*]

[a] Steacie Institute for Molecular Sciences, National Research Council of Canada, 100 Sussex Drive, Ottawa, ON Canada K1A 0R6

[b] Department of Chemistry, 560 Oval Drive, Purdue University, West Lafayette, Indiana 47907

Abstract

Supported membranes prepared from binary mixtures of DOPC and the bolalipid C_{20}BAS have been examined by atomic force microscopy (AFM). The supported membranes are phase separated to give a thicker DOPC-rich phase and a thinner bolalipid-rich phase for a range of lipid compositions. These results confirm an earlier prediction from mean field theory that phase separation is the thermodynamically stable state for membranes containing approximately equimolar C_{20}BAS and double chain monopolar lipids with chain lengths exceeding fifteen carbons. Hydrophobic mismatch between the monopolar lipid hydrocarbon chains and the membrane spanning bolalipid chains was suggested to provide the driving force for phase separation. The AFM results also show that the morphology of the mixed POPC:C_{20}BAS supported membranes varies significantly with the conditions used to prepare the vesicles and supported membrane samples. The complex membrane morphologies observed are attributed to the interplay of several factors, including a compositionally heterogeneous vesicle population, exchange of lipid between the vesicle solution and solid substrate during formation of the supported membrane, and slow equilibration of domains due to pinning of the lipids to the solid support.

Introduction

Bolalipids (a.k.a. bolaamphiphiles) are a class of bipolar lipids with two polar headgroups attached by one or more hydrocarbon chains. They comprise a significant fraction of the membrane lipids of *Archaea*, single cell organisms that have evolved to withstand harsh environmental conditions such as extreme temperatures, low pH, low oxygen tensions or high salt concentrations.[1–3] Membrane spanning alkyl chains of bolalipids[4, 5] are one of the most important structural factors responsible for the enhanced stability of archaeal membranes relative to bilayer membranes. The robust character of bolalipids has led to their use in a number of potential applications, including gene and vaccine delivery and the development of planar supported membranes for biosensors incorporating integral membrane proteins.[6–10] The difficulty and costs associated with the isolation of pure bipolar archaeal lipids in practical quantities has motivated the development of efficient pathways for bolalipid synthesis.[11–16]

Previous work has shown that bolalipid membranes are more stable and less permeable than conventional monopolar lipid membranes,[17] but still retain lateral mobilities that are similar

*Corresponding authors. davethom@purdue.edu; Linda.Johnston@nrc-cnrc.gc.ca.

to those of monopolar lipids.[18] Lipid lateral mobility and resistance toward delamination are important attributes for planar supported membranes in biosensing applications. Thompson and coworkers have recently synthesized three symmetric, acyclic bolalipids with glycerophospholine headgroups and bearing either 20 or 32 carbon transmembrane chains;[7, 11, 19] they have also characterized the lamellar thickness[5, 20] and fluidity[18] of these bolalipid membrane dispersions to evaluate their suitability for reconstitution of integral membrane proteins.[7, 8] This work showed that the activity of Ste14p, a yeast membrane-associated enzyme in the family of isoprenylcysteine carboxyl methyltransferases, varied with the length of the bolalipid alkyl chain and the POPC molar ratio when reconstituted in mixed bolalipid:POPC membranes.[7] Significantly lower protein activity was observed in C_{20}BAS membranes with low POPC content (i.e., < 30 mol%) relative to the longer chain analogue, C_{32}phytBAS.[7] These findings were attributed to hydrophobic mismatch between the C_{20}BAS bolalipid and the hydrophobic, membrane-spanning sequences of Ste14p. Enzyme activity increased significantly when the bilayer-forming lipid content exceeded ~30 mol% C_{20}BAS, however, fluorescence staining experiments provided no evidence of phase separation of either Ste14p from the vesicle membrane or the C_{20}BAS:POPC mixed membranes themselves on macroscopic length scales.

A recent theoretical study has used mean field theory to examine the structure and phase behavior of mixed monopolar lipid:bolalipid membranes.[21] The results predict that phase separation is the thermodynamically stable state of mixed membranes containing approximately equimolar C_{20}BAS and double chain monopolar lipids with chain lengths exceeding fifteen carbons (Figure 1). The driving force for phase separation into two liquid phases was attributed to hydrophobic mismatch between the monopolar lipid hydrocarbon chains and the membrane spanning bolalipid chains. When the hydrophobic mismatch is sufficiently large, two liquid phases were predicted, one thinner membrane phase enriched in bolalipid and a second thicker bilayer phase enriched in monopolar lipid. Since bolalipids are capable of adopting two conformations, a transmembrane conformation with the headgroups on opposing sides of the membrane and a U-shaped conformer with both headgroups on the same side of the membrane, it was not clear how C_{20}BAS would be arranged in mixed membrane dispersions. Longo et. al. predicted that the thinner domain would be enriched in bolalipids that are predominately in their transmembrane conformations, while the thicker, monopolar lipid-rich domain would contain a small population of bolalipids in U-shaped conformations (Figure 1). This prediction is consistent with experimental evidence reported for bolalipid systems. The ratio of looping to transmembrane conformers has been investigated by ^{2}H NMR for two phosphocholine-type bolalipids. A C_{28} bolalipid derivative was shown to exist with >90% transmembrane conformers;[4] similarly, C_{20}BAS showed no evidence for looping conformers at room temperature.[22] ^{2}H NMR spectra of POPC:C_{20}BAS mixtures with either perdeuterated POPC-d_{31} or bolalipid specifically labeled with deuterium in the middle of the transmembrane chain showed that two distinct liquid phases are detectable between POPC:C_{20}BAS ratios of 50:50 to 90:10.[5] It was further noted that (1) transmembrane conformers are the predominant species even at low fractions of bolalipid (e.g., 10 mol% C_{20}BAS) and (2) only a single lamellar thickness is detected by SAXS across the same range of compositions. Taken together, these findings provide strong evidence for the occurrence of microphase separated membranes in POPC:C_{20}BAS samples. This work, combined with the diffusion coefficient determined by pulsed field gradient NMR,[18] enabled an estimate of > 50 nm for the minimum domain radius in these dispersions.[5]

The theoretical prediction of phase separation for some C_{20}BAS:monopolar lipid membranes is consistent with experimental observations and computational studies of liquid-liquid phase separation for other fluid-phase phosphatidylcholine mixtures.[23, 24] It also raises the interesting possibility that domain formation may play a role in determining the activity of membrane proteins that have been reconstituted in bolalipid:POPC membranes or other non-native

membrane vesicle compositions. This is of practical importance for the development of bolalipid-stabilized supported membranes for biosensing applications. We sought to experimentally probe the role of hydrophobic mismatch between C_{20}BAS and POPC in pure C_{20}BAS bolalipid and mixed C_{20}BAS:POPC supported lipid membranes using atomic force microscopy (AFM). AFM has been widely used to probe domain formation in a variety of binary and ternary mixtures that exhibit mixtures of liquid-disordered and gel or liquid-ordered phases.[25, 26] This method has a number of advantages, including the ability to detect small height differences between coexisting membrane phases and the capacity to examine domains across a range of length scales from tens of nm to tens of μm in aqueous solution under physiological conditions, without the requirement for labeling. Our studies confirm that C_{20}BAS:POPC lipid mixtures are phase separated over a range of compositions. They also show that the morphology of the planar supported membranes varies significantly with the conditions used to prepare the vesicles and supported membrane samples. We conclude that three factors contribute to the complex membrane morphologies observed – (1) a compositionally heterogeneous vesicle population; (2) a non-uniform exchange of lipid between the bulk solution and solid substrate during supported membrane formation; and (3) a slow equilibration between the surface-supported domain structures due to pinning of the lipids to the underlying solid support.

Materials and Methods

Materials

C_{20}BAS was synthesized as described previously.[11, 19] 1-Palmitoyl-2-oleoylphosphatidylcholine (POPC) and 1,2-dimyristoylphosphatidylcholine (DMPC) were obtained from Avanti Polar Lipids and were used as received. All aqueous solutions were prepared with 18.3 MΩ·cm Milli-Q water. All other materials were obtained from Aldrich (≥98% pure) and used as received.

Preparation of Small Unilamellar Vesicles

Separate 5 mM chloroform stock solutions of POPC and C_{20}BAS were mixed in the appropriate ratios, the solvent was removed and the film was dried under vacuum overnight. The lipid films were then hydrated in water and vortexed to obtain multilamellar vesicles. Vesicles were formed either by sonication or extrusion. Sonicated samples were prepared from the multilamellar vesicles using a bath sonicator with an initial temperature of 20 °C (or between 20–60 °C, as noted in the text) to form clear dispersions of small unilamellar vesicles with a final lipid concentration of 1mg/mL. Extruded vesicles were formed by passing multilamellar vesicle suspensions (250 μL) 11 times through polycarbonate membranes with pore sizes of 100, 200 or 400 nm using a Liposofast extruder. Vesicles were used immediately after their formation for the preparation of supported membranes.

Preparation of Supported Membranes

An aliquot of vesicle solution (50 μL) and Milli-Q water (400 μL) were added to freshly cleaved mica clamped into a Molecular Imaging AFM liquid cell. After incubation at room temperature for 3 hours, the bilayers were rinsed extensively with Milli-Q water to remove unattached vesicles before imaging. Scanning at high force with the AFM tip over a small area in MAC-mode to create a bilayer defect allowed us to measure the bilayer thickness, confirming the presence of a single bilayer. For higher incubation temperatures, samples were incubated at the desired temperature for 2 hours and then cooled to room temperature at a rate of 20 °C/h. In some experiments membranes were prepared on n-type silicon (111) wafers polished on one side with a thickness of 250 ± 25um and a resistance of 1.0–5.0 Ohm•cm. The silicon was cleaned using a standard piranha solution (3:1 sulfuric acid:hydrogen peroxide; CAUTION:

piranha solutions are potentially explosive!) for 20 minutes at 120 °C. The wafers were then rinsed using copious amounts of Milli-Q water and stored in water until further use.

Atomic Force Microscopy

The AFM images were obtained at room temperature (22 ± 1 °C) using a PicoSPM atomic force microscope (Molecular Imaging) in MAC-mode. Magnetic coated silicon tips with spring constants of ~0.5 N/m and resonance frequencies between 5 and 40 kHz in aqueous solution were used. A 30 × 30 μm^2 scanner was operated at a scan rate between 0.7 and 1.3 Hz. The images shown are flattened raw data. Two or more independently prepared samples were imaged for each bilayer composition with several areas scanned for each sample. Reported heights are based on averaging data for at least two independent samples with a minimum of 9 areas imaged.

Dynamic Light Scattering

Vesicle samples were diluted, typically ~1:10, with Milli-Q water prior to DLS measurements. Vesicle size distributions were determined using a Nicomp Model 370 Laser Particle Sizer (Nicomp Instruments, Santa Barbara, CA) which utilized a measurement angle of 90° and a 5 mW Ne laser operating at 632.8 nm.

Cryo-TEM

C_{20}BAS:POPC liposomes (1:1 mol:mol, 30 mM total lipid concentration) were extruded 11 times through 200 nm track-etch membranes. The liposome solution was then transferred by pipet to a bare Quantifoil grid, the excess blotted away using filter paper, and the sample vitrified in liquid ethane slush cooled by liquid nitrogen. The grid was then transferred to a Philips CM200 transmission electron microscope equipped with a liquid nitrogen-cooled stage and a field-emission gun operating at 200 kV accelerating voltage. The cryoTEM images were collected at 50,000× magnification under low dose conditions to minimize radiation damage to the samples.

Results

AFM Characterization of POPC and C_{20}BAS Membranes

AFM images of samples formed by incubating two different concentrations of sonicated POPC vesicles on mica for 1 hour, followed by washing to remove excess vesicles, produced bilayer patches and continuous bilayers as shown in Figure 2A & B. At low lipid concentrations, there are many small bilayer patches with a height of 4.0 nm, while at higher lipid concentrations, a uniform, featureless bilayer membrane is formed. Noticeably longer incubation times were required to produce supported membranes from C_{20}BAS vesicles at the same lipid concentration. Figure 2C shows large patches of C_{20}BAS bolalipid membrane, with a thickness of 2.7 ± 0.4 nm, formed with an incubation time of ~ 3 days. A smaller area with a continuous membrane in which a small area was scanned at high force to create a defect is shown in the insert of Figure 2C. The measured thickness is consistent with the measured lamellar repeat distance of 32 Å by small angle x-ray scattering.[20, 21] Shorter incubation times gave either small membrane patches or adsorbed vesicles that were very difficult to image.

AFM Characterization of POPC:C_{20}BAS Membranes

Vesicles with mixtures of POPC and C_{20}BAS across a range of molar ratios were prepared by sonication and used to form supported membranes for AFM characterization. The results are shown in Figure 3. Uniform, featureless images were obtained for samples with 0.1 and 0.9 mol fractions of C_{20}BAS (X_B) after incubation for 3 hours. The X_B = 0.9 sample was scanned at high force to create a defect and verify that there was an intact membrane on the mica surface;

however, it was not possible to maintain a defect in the $X_B = 0.1$ sample, presumably because the highly abundant monopolar POPC lipids are sufficiently mobile to rapidly refill defects created by the tip, as is commonly observed for fluid POPC bilayers. AFM images of samples prepared from vesicles with $X_B = 0.6$, 0.5 and 0.4 all showed evidence of phase separation, with domains of thicker and thinner membrane regions apparent. For $X_B = 0.6$, there were a number of small raised islands that were 1.2 ± 0.2 nm higher than the surrounding lower phase (Figure 3B). The islands ranged in size from 10–15 nm in diameter and covered 6 ± 2 % of the surface area. Qualitatively similar results were obtained for $X_B = 0.5$, but both the number and size of the small raised islands increased; most of the islands ranged from 50 to 100 nm in diameter and there were a few larger features that appeared to be formed by coalescence of small adjacent islands (Figure 3C). The islands were 1.9 ± 0.2 nm higher than the surrounding lower phase and covered 22 ± 2 % of the surface. The morphology was significantly different for $X_B = 0.4$, with a number of small lower areas (depth of 1.0 ± 0.1 nm) that were surrounded by a uniform membrane. Scanning at high force to create a defect indicated that there was an intact membrane with small regions of lower phase, as opposed to an incomplete membrane with areas of bare mica. The higher phase covered 86 ± 2% of the surface. The overall membrane morphology, including the size and depth of the small regions of lower phase, did not change over a period of 24 hours. Similarly, no change in morphology was observed when a sample with $X_B = 0.5$ was imaged before and after heating at 40 °C for 1 hour, followed by cooling.

Based on the measured thickness of pure POPC and C_{20}BAS membranes, it is reasonable to assign the higher phase observed for the lipid mixtures to a POPC-rich phase and the lower regions to a bolalipid-rich phase. This is also consistent with the observation that the amount of the higher phase decreases with increasing mole fraction of C_{20}BAS. However, the surface coverage data does not follow a uniform trend with increasing POPC concentration. If one assumes that the area/molecule is similar for POPC and C_{20}BAS in the transmembrane configuration[11], then there is more C_{20}BAS phase than expected for $X_B = 0.6$ and 0.5 mixtures and less for the $X_B = 0.4$ mixture.

For comparison, membranes were prepared by physically mixing pure C_{20}BAS bolalipid and pure POPC vesicles before immediately incubating the vesicle mixture with mica, using the same conditions as for the samples in Figure 3. AFM images for both $X_B = 0.5$ and 0.4 showed small raised islands randomly distributed throughout the sample (see Figure 2F for $X_B = 0.5$). The surface coverage of the raised islands was 18 ± 2% and 26 ± 2% for X_B =0.5 and 0.4, respectively, and in both cases the islands were 2.3 ± 0.1 nm higher than the surrounding membrane. By analogy to the results above, we assign these islands to a POPC-rich phase. The relatively low fraction of the surface covered by the POPC-rich islands is surprising based on the very different incubation times required to form membranes from pure POPC and pure C_{20}BAS vesicles. Since POPC vesicles give a continuous bilayer with considerably lower lipid concentrations and shorter incubation times, one might have predicted the formation of a predominantly POPC bilayer from the physical mixture of vesicles. Interestingly, the morphologies for $X_B = 0.5$ are very similar when membranes are formed using either a physical mixture of pure lipid vesicles or vesicles with premixed lipids. By contrast, quite different results are obtained for the two methods for $X_B = 0.4$.

Diameters for sonicated vesicles were determined by dynamic light scattering and the results are summarized in Table 1. C_{20}BAS vesicles had a significantly smaller mean diameter, 24 nm, than either POPC or POPC:C_{20}BAS vesicles, all of which had mean diameters between 40–45 nm.

Effects of Vesicle Preparation and Incubation Conditions on Membrane Morphology

The size and shape of membrane domains and the kinetics for supported bilayer formation are affected by a variety of factors. These include (1) the size, net charge, lipid composition and concentration of the vesicles; (2) the aqueous environment present in the mica cell during vesicle adsorption and rupture; and (3) the characteristics of the solid support.[27, 28] We hypothesized that the unusual trend in the ratios of higher and lower phases with changing lipid ratios could reflect a heterogeneous population of vesicles in the dispersed samples, with a significant fraction of the vesicles possessing lipid ratios that are different from the bulk composition. If this were true, the process of vesicle adsorption and rupture on the surface could favor a specific vesicle population, thus leading to a membrane that does not reflect the nominal lipid ratios. An alternate possibility is that lipid exchange between the surface and vesicles occurs during supported membrane formation, thus leading to significant differences in composition between the final supported membrane and the initial vesicles. We carried out a number of experiments to further investigate these possibilities.

First, we examined the effects of vesicle sonication conditions on membrane morphology. We found no change in membrane morphology for samples prepared with $X_B = 0.4$ vesicles sonicated using several different protocols (e.g., variable times, bath vs. probe sonicator, or sonication temperatures between 20 and 60 °C). It should be noted that the gel to liquid-crystalline phase transition temperatures of POPC and C_{20}BAS are −2 °C and 17 °C, respectively;[7] therefore, both lipids are in the fluid phase over the temperature range investigated. Vesicles sonicated at 56 °C gave supported membranes with a different morphology featuring small raised areas that were 1.1 nm above the surrounding lower regions of the membrane. There were also occasional dark defects, indicating close to complete membrane coverage, although the defects were not large enough to obtain a reliable depth measurement. Increasing the incubation temperature from 20 to 60 °C for vesicles sonicated at room temperature also produced a change in membrane morphology (Figure 4A & B). The higher resolution image (Figure 4B) shows that this sample has three distinct heights, with small and irregularly-shaped regions that are either 2.5 or 4 nm above the lowest (dark) regions that are assigned to exposed mica between membrane defects.

Second, we probed the effect of vesicle size by using extrusion to make vesicles of controlled sizes. Multilamellar vesicles prepared by hydrating lipid films with $X_B = 0.4$, 0.5 and 0.6 were extruded through a 100 nm filter, giving vesicles with mean diameters of 71, 127 and 104 nm, respectively. Vesicles with $X_B = 0.4$ produced phase separated membranes with raised domains (1.6 ± 0.2 nm higher than the surrounding lower phase) with a wide distribution of sizes and shapes (Figure 4C). The surface coverage of the domains varied significantly from area to area of the same sample, with an average value of 30% for 4 large images (>10 × 10 μm^2) for the sample shown in Figure 4C. They also varied from sample to sample, displaying in some cases smaller domains that covered a significantly lower fraction of the surface (7%). Membranes prepared from $X_B = 0.4$ extruded vesicles using lower lipid concentrations (~10 times less) showed qualitatively similar phase separation. By contrast, extruded vesicles with $X_B = 0.5$ and 0.6 formed featureless bilayers (data not shown).

Vesicles with $X_B = 0.4$ were also extruded through filters with pores sizes of 200 nm and 400 nm to give vesicles with a mean diameter of 120 and 150 nm, respectively. Both samples gave phase separated membranes that showed an increased number of small domains as compared to samples prepared from vesicles with a smaller mean diameter (71 nm) as shown in Figure 4C. Surface coverages of the raised domains are 35 ± 2 % and 35 ± 3 % for samples prepared by extrusion through 200 and 400 nm filters, respectively.

A final experiment investigated the effect of substrate on the appearance of the supported membranes. Mica was replaced with silicon for sonicated vesicle samples containing $X_B = 0.5$

and the resulting supported membranes imaged by AFM. Figure 4D shows a supported membrane image on silicon (111); there are many small islands (30–60 nm in diameter) that are 1.6 ± 0.2 nm above the lower phase and that cover 20 ± 1.6% of the surface, similar to the result on mica.

Cryo-TEM of POPC:C_{20}BAS Vesicles

Cryo-TEM was utilized to examine the morphology of POPC:C_{20}BAS vesicles (X_B = 0.5) prepared by both sonication and extrusion with a 200 nm pore size filter. Representative cryo-TEM images of sonicated vesicles (measured 3 days after preparation) are shown in Figure 5A & B. This sample was heterogeneous with some areas having a distribution of vesicle sizes ranging from 10–70 nm in diameter (Figure 5A), consistent with the light scattering results, while other areas had much larger vesicles, some of which were elliptical in shape, as well as membrane fragments (Figure 5B). The larger structures presumably arise from fusion of smaller vesicles as has been previously reported for extruded bolalipid dispersions.[20] By contrast, cryo-TEM of extruded vesicles (X_B = 0.5) showed a range of vesicle sizes between 30–200 nm, but no evidence for the larger vesicles or membrane fragments observed for the sonicated vesicles (Figure 5C & D). Interestingly, thicker and thinner regions of the membrane could be clearly distinguished for some of the larger extruded vesicles (see arrows in Figures 5C & D). This is consistent with the presence of POPC-rich and C_{20}BAS bolalipid-rich regions within the same vesicle.

AFM Characterization of DMPC:C_{20}BAS Membranes

Supported membranes on mica were also prepared for a DMPC:C_{20}BAS mixture (X_B = 0.4) using both sonicated and extruded (100 nm filter) vesicles. Sonicated vesicles gave a featureless lipid bilayer (Figure 6A). By contrast, the supported membrane produced from extruded vesicles had large raised domains (2.2 ± 0.2 nm) surrounded by a uniform lower phase, Figure 6B. The domains were interconnected, with irregular perimeters and covered 64 ± 4% of the sample.

Discussion

The AFM results demonstrate that POPC:C_{20}BAS mixtures phase separate to give thicker POPC-rich and thinner C_{20}BAS-rich regions across a range of compositions in supported membranes on solid substrates, an observation that is qualitatively confirmed by cryo-TEM data for their binary lipid mixtures. This is consistent with previous computational and experimental findings that membranes comprised of C_{20}BAS and monopolar lipids with significantly different hydrocarbon chain lengths undergo phase separation due to hydrophobic mismatch.[5, 21] The earlier computational study predicted that phase separated membranes would be obtained for approximately equimolar mixtures of bolalipid and monopolar lipids with chain lengths greater than 15 carbons. The calculated miscibility diagram further indicated that mixtures of C_{20}BAS with a C_{18} monopolar lipid would be phase-separated between 20–80 mol% bolalipid, in remarkably good agreement with the AFM results that we obtained for POPC:C_{20}BAS membranes.[21]

Although POPC-bolalipid membranes exhibit clear phase separation, there are a number of puzzling aspects for the morphologies obtained using different sample preparation methods. First, although the C_{20}BAS bolalipid-rich phase area generally increases with increasing bolalipid content for bilayers prepared from sonicated vesicles, the surface coverage does not follow a uniform trend. Assuming that the area/molecule is similar for both lipids[11], there is more C_{20}BAS bolalipid-rich phase than expected for X_B = 0.6 and 0.5 mixtures and less for the X_B = 0.4 mixture. Second, the membrane morphology (i.e., the size and shape of the POPC-rich domains and their fractional surface coverage) for some lipid mixtures varies significantly

with temperature and with the method of preparation of the vesicles and the supported membranes. One possible explanation for these observations is that the composition of the supported membranes may be significantly different from that of the initial vesicles for some of the sample preparation methods. A change in lipid ratio between the bulk vesicle population and the substrate-supported membrane could occur during membrane formation, either by selective deposition of a compositionally-heterogeneous vesicle sub-population or by exchange between the developing surface-supported membrane and the bulk vesicle solution. Some of the variation in domain morphology may also reflect slow membrane equilibration. The role of these factors in determining the complex morphologies for POPC:C_{20}BAS supported membranes is discussed below.

Formation of supported bilayers from unilamellar vesicles on glass and mica has been studied in detail using AFM and quartz crystal microbalance techniques.[27, 28] Following adsorption to the surface, vesicles can (1) remain intact on the surface, eventually giving a layer of adsorbed vesicles; (2) rupture rapidly giving small bilayer disks that then merge with other bilayer patches or promote rupture of adjacent vesicles, eventually forming a continuous membrane; or (3) fuse to give larger vesicles before rupturing to give bilayer patches. The stability of individual adsorbed vesicles depends on their size, lipid composition, solution composition (particularly the presence of divalent cations) and the properties of the surface.

A heterogeneous population of vesicles will lead to a bilayer that does not reflect the bulk lipid composition if one vesicle population adsorbs and ruptures to form membrane patches more rapidly than another. Small unilamellar vesicles prepared by either sonication or extrusion have been used extensively for the preparation of supported bilayers from multi-component lipid mixtures, in most cases with the implicit assumption that both individual vesicles and the supported bilayer have the same lipid ratio as the bulk vesicle solution. However, compositional heterogeneity of vesicles has been reported in some cases. For example, giant unilamellar vesicles prepared from ternary lipid mixtures with co-existing liquid phases occasionally show a mixture of vesicles with and without phase coexistence by fluorescence microscopy; these results have been attributed to differences in lipid composition between vesicles.[29] Similarly, a study of ternary lipid mixtures has concluded that lipid demixing leads to changes in phase diagrams when the vesicle samples are prepared by different methods.[30] It has been suggested that lipid demixing artifacts may be particularly problematic for cholesterol-rich mixtures. The presence of C_{20}BAS bolalipid, which can exist in both transmembrane and U-shaped conformers, may also promote lipid demixing when significant hydrophobic mismatch is present, resulting in a heterogeneous population of vesicles.

The unexpected trends in the percentages of C_{20}BAS-rich surface coverage with increasing bolalipid content for membranes prepared from sonicated vesicles could be partially due to a heterogeneous population of vesicles with different POPC:C_{20}BAS ratios that possess different intrinsic rates of supported membrane formation. Consistent with this hypothesis, pure POPC vesicles form a continuous membrane much more rapidly than do pure C_{20}BAS vesicles. This can be attributed to the fact that the C_{20}BAS vesicles were smaller than the critical radius for vesicle adsorption and rupture reported for unilamellar vesicles of fluid phosphatidylcholines (PC).[31] This study showed that isolated vesicles with radii <25 nm remained intact on mica, whereas larger vesicles (>75 nm) rapidly ruptured to form bilayer disks. At high lipid concentrations, formation of a supported bilayer from small vesicles (<75 nm) was shown to proceed by fusion of vesicles to give larger vesicles that rupture on the surface. Although cryo-TEM images provide evidence for membranes with two different thicknesses for some larger vesicles, they do not allow us to address the questions of compositional variation in the smaller vesicle population or in the supported membrane itself.

Variations in preparation methods for sonicated vesicles gave consistent membrane morphologies in most cases. However, heating the samples above 50 °C during either sonication or incubation did show some differences. Although membranes were still phase separated, the surface coverage of POPC-rich and C_{20}BAS-rich domains was different and more membrane defects were apparent. These changes may be due to a higher contribution of the bolalipid U-shaped conformer at higher temperature, consistent with the observations reported in ^{2}H NMR studies of POPC:C_{20}BAS mixtures.[5] In spite of the increased population of U-shaped conformers that occurs at elevated temperatures, ^{2}H NMR results showed that these conformers were capable of relaxing into the transmembrane conformation upon cooling the vesicle dispersion to room temperature. This relaxation process may be more difficult, however, for supported membranes that may possess a significant fraction of pinned lipids.

The morphology of membranes prepared from extruded POPC:C_{20}BAS vesicles was significantly different from that obtained for sonicated vesicles with $X_B = 0.4$, with a much lower coverage of the POPC-rich phase and the formation of relatively large domains. POPC:C_{20}BAS membranes prepared from extruded vesicles with $X_B = 0.5$ and 0.6 were also significantly different than those for the corresponding sonicated samples, with small islands of POPC-rich phase present in the sonicated vesicle samples, but uniform featureless membranes arising from extruded vesicle samples. Heterogeneous sizes and compositions of vesicles prepared by sonication and extrusion may partially account for these results.

Several observations indicate, however, that vesicle heterogeneity is unlikely to be the only factor that contributes to the complex sample morphologies that were observed for POPC:C_{20}BAS supported membranes. For example, there is a larger fraction of the C_{20}BAS bolalipid-rich phase than expected for $X_B = 0.6$ and 0.5 mixtures and less for the $X_B = 0.4$ mixture. This cannot be explained simply by POPC-rich vesicles forming a membrane more rapidly than bolalipid-rich vesicles. Furthermore, the 1:1 physical mixture of pure POPC and pure C_{20}BAS vesicles would be expected to give a predominantly POPC membrane, based on the faster kinetics for membrane formation from POPC vesicles. The observation of a supported membrane with a relatively small fraction of POPC-rich phase requires a mechanism for lipid scrambling, either by rapid fusion of small adsorbed vesicles to produce larger vesicles that rupture to give membrane patches or by lipid exchange between the surface and vesicles in solution during or after membrane formation. In this regard, neutron diffraction studies have shown that DOPC:DPPC bilayers on silica have a substantially different composition from the bulk vesicles, with an enrichment of DPPC in the lower leaflet.[32] These results were attributed to exchange of material between the surface bilayer and the bulk vesicle solution during bilayer formation. In agreement with this hypothesis, lipid exchange between small unilamellar vesicles containing charged lipids and supported bilayers has also been observed.[33, 34] It is plausible that adsorbed C_{20}BAS vesicles undergo an accelerated fusion and planar surface deposition that is facilitated by the presence of the more dynamic POPC component.

In most cases, the domains for POPC:C_{20}BAS membranes are small (<100 nm) and do not coalesce to give larger domains when the membrane is stored at room temperature for 1 day or is heated to 50 °C. The observed domain size is consistent with the estimates of >50 nm from NMR and SAXS data for POPC C_{20}BAS dispersions.[5] However, these results differ from data for a variety of phase-separated bilayers composed of binary and ternary lipid mixtures, which typically have domain sizes ranging from several hundred nanometers up to tens of micrometers.[25, 26] Domain sizes are determined by the balance between entropy, line tension at the domain perimeter and long-range dipole-dipole repulsion. Several recent studies have demonstrated that line tension increases with increasing hydrophobic mismatch between the domain and the surrounding membrane, and decreases in the presence of cholesterol.[35–37] A quantitative model for creation and evolution of domains in multicomponent bilayers predicts that for sufficiently small line tensions (1) the decrease in the entropy term that results from

domain merger is larger than the decrease in boundary energy and (2) nanodomains are in quasi-equilibrium and do not increase in size. [38, 39] At high line tension, however, nanodomains rapidly merge to give larger micron-sized domains because the decrease in boundary energy dominates the unfavorable entropy of merger. Based on the dependence of line tension on hydrophobic mismatch for binary and ternary lipid mixtures,[36, 37, 40] the >1 nm hydrophobic mismatch for C_{20}BAS/POPC mixtures would be predicted to give a relatively high line tension, thus favoring large domain size. This contrasts with our results for POPC:C_{20}BAS membranes prepared from sonicated vesicles, although it is not clear if one can extrapolate line tension behavior from bilayer membrane lipid mixtures to bolalipid membranes with predominantly transmembrane conformations.

An alternate possibility is that pinning of the bolalipid to the support prevents equilibration and limits the domain size. Coupling of domains to the surface is affected by the ionic strength of the aqueous medium, with the presence of salts helping to decouple the bilayer from the underlying support.[41, 42] Bilayers are frequently prepared in the presence of Ca^{2+}, which promotes vesicle rupture and may reduce pinning of the lipids to the underlying support. We have avoided the use of Ca^{2+} in these experiments since it may affect the equilibrium between transmembrane and U-shaped bolalipid conformers in a manner that is not presently understood. This choice may have contributed to increased pinning of individual lipids onto the solid substrate, thereby resulting in small domains for sonicated vesicles and irregular domain boundaries for membranes prepared from larger extruded vesicles. It is also possible that the formation of featureless membranes for some samples reflects very slow domain nucleation and growth from POPC:C_{20}BAS supported membranes, so that a membrane containing both lipids does not appear phase-separated, even at the spatial resolution of AFM. This is consistent with the expectation that domain growth may be slower for transmembrane bolalipids than for monopolar lipids.

Finally, we have shown that DMPC:C_{20}BAS membranes ($X_B = 0.4$) produce qualitatively similar results to those for POPC:C_{20}BAS, with phase-separated and apparently uniform membranes observed for extruded and sonicated vesicles, respectively. The similar behavior for phosphatidylcholine lipids with either saturated or unsaturated hydrocarbon chains could indicate that pinning of the lipid head groups is a dominant factor in controlling membrane morphology. Nevertheless, the large difference between sonicated and extruded vesicles argues for involvement of vesicle heterogeneity and/or lipid exchange, and we hypothesize that the same factors are responsible for variations in morphology of membranes prepared from mixtures of C_{20}BAS bolalipid with either POPC or DMPC.

Conclusions

Phase separated membranes prepared from mixtures of POPC and C_{20}BAS bolalipid have been examined in detail by AFM. The results indicate that the membrane morphology varies significantly for these samples as a function of the methods used to prepare vesicles and supported membranes. We infer from our findings that the membrane lipid composition is different from that of the bulk vesicle solution for at least some of the sample preparation methods, leading to complex changes in membrane morphology. Further experiments are needed to discern whether the ratios of monopolar lipid and bolalipid are changing during the deposition process and whether appreciable partial mixing of the lipids in the phase separated state is occurring. It is conceivable that processes involving selection of a subset of vesicles from an initial compositionally heterogeneous vesicle sample and exchange of lipid between the solid surface and the bulk solution may also be occurring during membrane formation to contribute to the observed effects. Finally, the small domain size obtained for some samples probably reflects pinning of lipids to the support, resulting in slow sample equilibration. This complex interplay of factors means that it is quite difficult to control the morphology of

supported membranes prepared from POPC:C_{20}BAS mixtures, an important observation in the context of applications of bolalipid mixtures for membrane biosensing. Whether this is related to the large hydrophobic mismatch between POPC and C_{20}BAS or is an inherent property of transmembrane bolalipids remains to be determined.

Acknowledgments

The authors thank Jessica Grey and Valorie Bowman for their assistance with the cryoTEM analysis and Dr. Maohui Chen for AFM assistance. LJJ acknowledges partial support of this work from the Natural Sciences and Engineering Research Council. DHT gratefully acknowledges the support of this work by NIH CA112427.

References

1. Koga Y, Morii H. Biosci Biotech Biochem 2005;69:2019.
2. Gambacorta A, Trincone A, Nicolaus B, Lama L, DeRosa M. Syst Appl Microbiol 1994;16:518.
3. Gliozzi A, Relini A, Chong PLG. J Memb Sci 2002;206:131.
4. Cuccia LA, Morin F, Beck A, Hebert N, Just G, Lennox RB. Chem Eur J 2000;6:4379–4384.
5. Brownholland DP, Longo GS, Struts AV, Justice MJ, Szleifer I, Petrache HI, Brown MF, Thompson DH. Biophys J 2009;97:2700–2709. [PubMed: 19917223]
6. Cornell BA, Braach-Maksvytis VLB, King LG, Osman PDJ, Raguse B, Wieczorek L, Pace RJ. Nature 1997;387:580. [PubMed: 9177344]
7. Febo-Ayala W, Moreira-Felix SL, Hrycyna CA, Thompson DH. Biochem 2006;45:14683–14696. [PubMed: 17144661]
8. Kim JM, Patwardhan A, Bott A, Thompson DH. Biochim Biophys Acta 2003;1617:10–21. [PubMed: 14637015]
9. Schiller SM, Naumann R, Lovejoy K, Kunz H, Knoll W. Angew Chem Int Ed Engl 2003;42:208–211. [PubMed: 12532352]
10. Sun XL, Biswas N, Kai T, Dai Z, Dluhy RA, Chaikof EL. Langmuir 2006;22:1201–1208. [PubMed: 16430284]
11. Patwardhan AP, Thompson DH. Langmuir 2000;16:10340–10350.
12. Patwardhan AP, Thompson DH. Org Lett 1999;1:241–244. [PubMed: 10905869]
13. Benvegnu T, Brard M, Plusquellec D. Curr Opin Coll Interface Sci 2004;8:469.
14. Kim JM, Thompson DH. Langmuir 1992;8:637–644.
15. Montier T, Benvegnu T, Jaffres PA, Yaouanc JJ. Curr Gene Ther 2008;8:296. [PubMed: 18855628]
16. Thompson DH, Wong KF, Humphry-Baker R, Wheeler JJ, Kim JM, Rananavare SB. J Am Chem Soc 1992;114:9035–9042.
17. Melikyan GB, Matinyan NS, Kocharov SL, Arakelian VB, Prangishvili DA. Biochim Biophys Acta 1991;1068:245. [PubMed: 1911833]
18. Febo-Ayala W, Holland DP, Bradley SA, Thompson DH. Langmuir 2007;23:6276–6280. [PubMed: 17465580]
19. Svenson S, Thompson DH. J Org Chem 1998;63:7180–7182. [PubMed: 11672358]
20. DiMeglio C, Rananavare SB, Svenson S, Thompson DH. Langmuir 2000;16:128–133.
21. Longo GS, Thompson DH, Szleifer I. Biophys J 2007;93:2609–2621. [PubMed: 17573422]
22. Holland DP, Struts AV, Brown MF, Thompson DH. J Am Chem Soc 2008;130:4584–4585. [PubMed: 18348566]
23. Lehtonen JYA, Holopainen JM, Kinnunen PKJ. Biophys J 1996;70:1753–1760. [PubMed: 8785334]
24. Longo GS, Schick M, Szleifer I. Biophys J 2009;96:3977–3986. [PubMed: 19450469]
25. Connell SD, Smith A. Mol Memb Biol 2006;23:17–28.
26. Johnston LJ. Langmuir 2007;23:5886–5895. [PubMed: 17428076]
27. Richter RP, Berat R, Brisson AR. Langmuir 2006;22:3497–3505. [PubMed: 16584220]
28. Goksu EI, Vanegas JM, Blanchette CD, Lin WC, Longo ML. Biochim Biophys Acta 2009;1788:254–266. [PubMed: 18822269]

29. Veatch SL, Keller SL. Biochim Biophys Acta 2005;1746:172–185. [PubMed: 16043244]
30. Buboltz JT, Bwalya C, Williams K, Schutzer M. Langmuir 2007;23:11968–11971. [PubMed: 17949025]
31. Reviakine I, Brisson A. Langmuir 2000;16:1806–1815.
32. Wacklin HP, Thomas RK. Langmuir 2007;23:7644–7651. [PubMed: 17539662]
33. Reinl HM, Bayerl TM. Biochem 1994;33:14091–14099. [PubMed: 7947819]
34. Callow P, Fragneto G, Cubitt R, Barlow DJ, Lawrence MJ, Timmins P. Langmuir 2005;21:7912–7920. [PubMed: 16089400]
35. Baumgart T, Hess ST, Webb WW. Nature 2003;425:821–824. [PubMed: 14574408]
36. Blanchette CD, Lin WC, Orme CA, Ratto TV, Longo ML. Biophys J 2008;94:2691–2697. [PubMed: 18065459]
37. Garcia-Saez AJ, Chiantia S, Schwille P. J Biol Chem 2007;282:33537–33544. [PubMed: 17848582]
38. Frolov VAJ, Chizmadzhev YA, Cohen FS, Zimmerberg J. Biophys J 2006;91:189–205. [PubMed: 16617071]
39. Kuzmin PI, Akimov SA, Chizmadzhev YA, Zimmerberg J, Cohen FS. Biophys J 2005;88:1120–1133. [PubMed: 15542550]
40. Blanchette CD, Lin WC, Orme CA, Ratto TV, Longo MJ. Langmuir 2007;23:5875–5877. [PubMed: 17451264]
41. Jensen MH, Morris EJ, Simonsen AC. Langmuir 2007;23:8135–8141. [PubMed: 17590026]
42. Seeger HM, Marino G, Alessandrini A, Facci P. Biophys J 2009;97:1067–1076. [PubMed: 19686654]

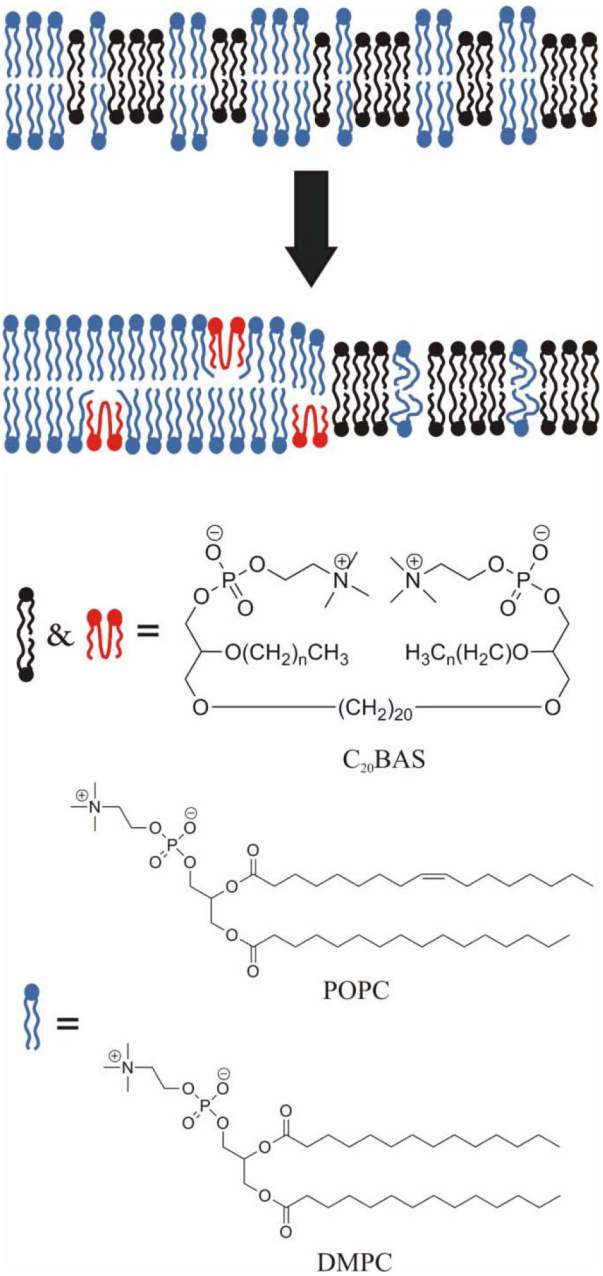

Figure 1.

Structures of C_{20}BAS, POPC and DMPC. The cartoon shows phase separation for a mixed C_{20}BAS/PC lipid membrane to give thinner domains that are predominantly transmembrane bolalipids and thicker domains that are enriched in monopolar lipid and have a small fraction of bolalipid U-conformers.

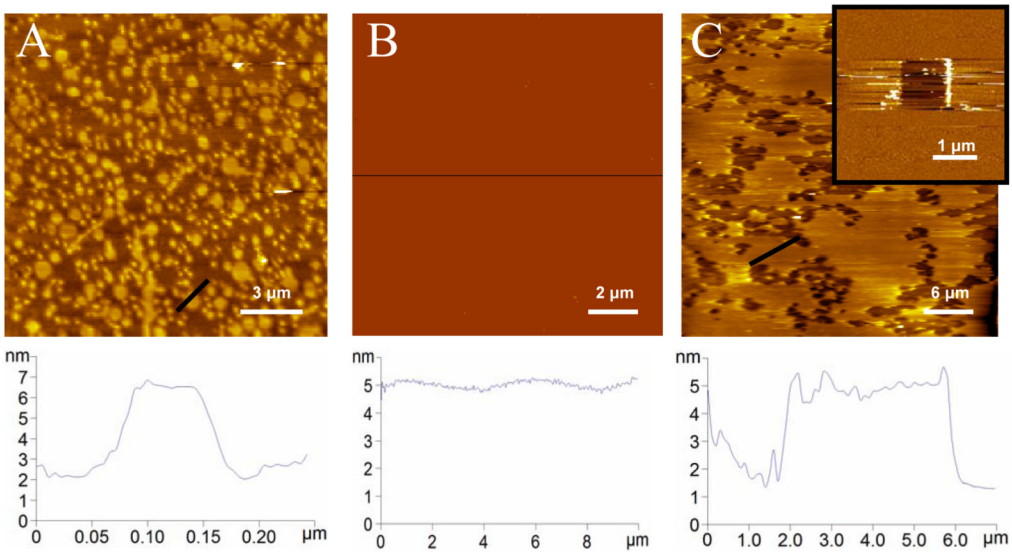

Figure 2.

AFM images of POPC and C_{20}BAS supported membranes prepared from sonicated vesicles at room temperature on mica. (A) POPC patches and (B) a continuous bilayer formed by incubating 3 μg and 50 μg total lipid for 1 hour. (C) C_{20}BAS membrane patches produced by incubating 50 μg total lipid for 72 hours; the insert shows an area of continuous membrane for a different sample for which a small region was scanned at high force to create a persistent defect. Cross sections for the lines marked on each image are shown below the images.

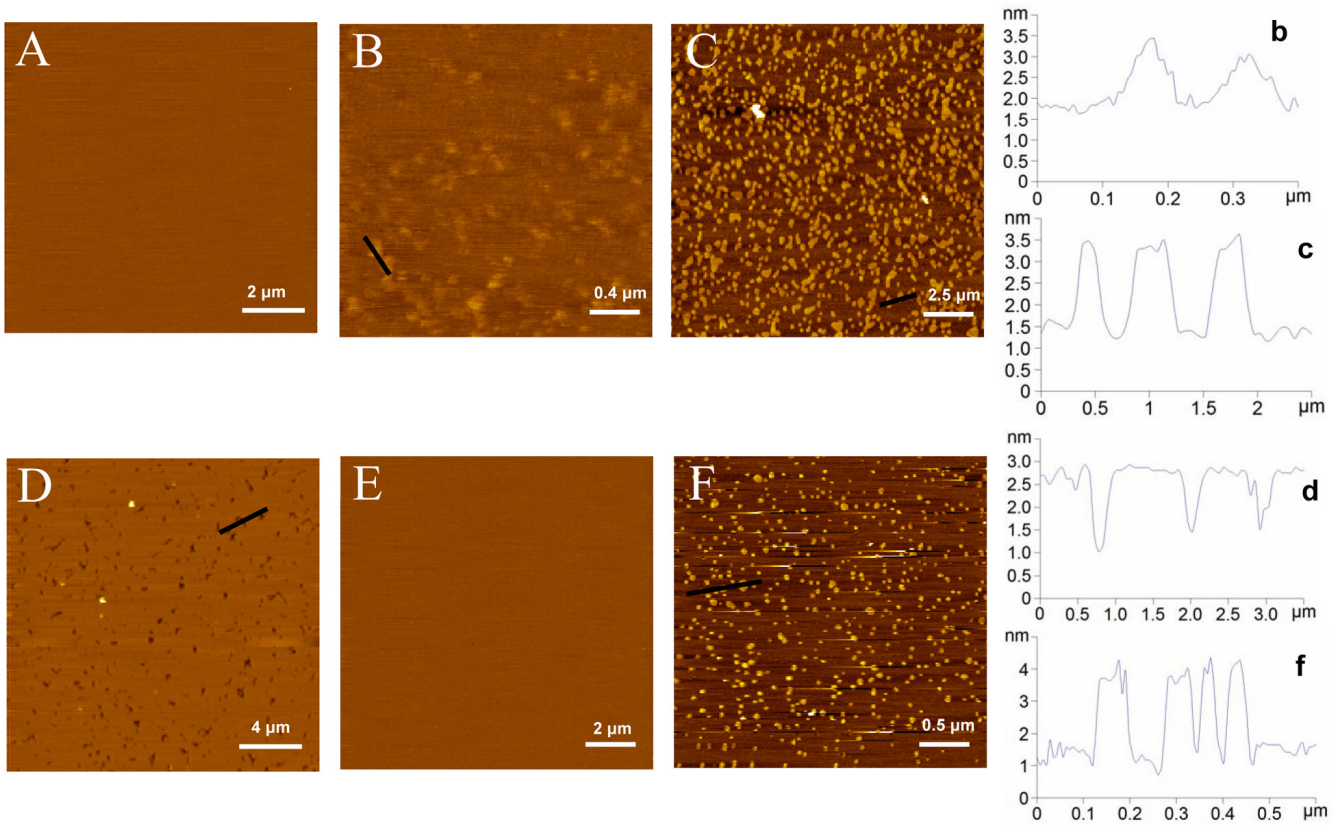

Figure 3.

(A–E) AFM images of supported membranes prepared from sonicated vesicles with various POPC:C_{20}BAS ratios. Images A–E are for X_B = 0.9, 0.6, 0.5, 0.4 and 0.1, respectively. Image F shows a supported membrane prepared by mixing pure POPC and pure C_{20}BAS sonicated vesicles (1:1 ratio) immediately before exposure to the mica substrate. Cross sections for the lines marked on images B, C, D and F are shown on the right.

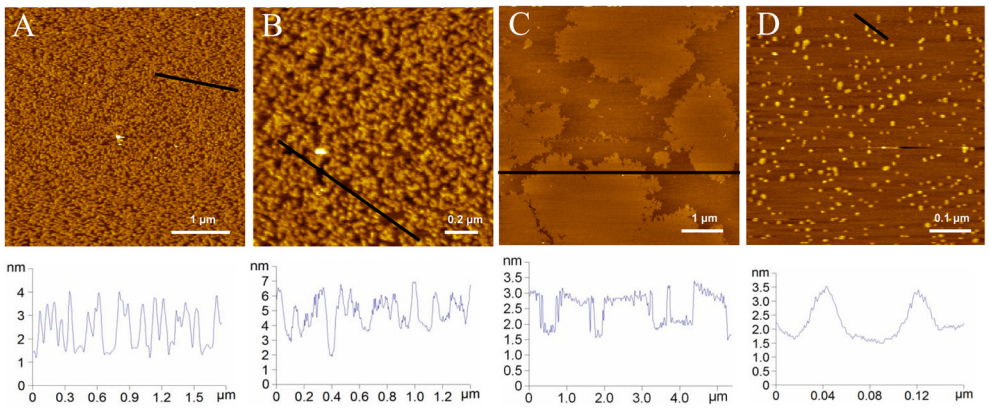

Figure 4.

(A, B) AFM images of supported membranes prepared from sonicated vesicles (POPC:C_{20}BAS, X_B = 0.4) after incubation at 60°C on mica. (C) AFM images of supported membranes prepared from extruded vesicles (POPC:C_{20}BAS, X_B = 0.4, mean vesicle diameter = 71 nm) on mica at room temperature. (D) AFM images of supported membranes prepared from sonicated vesicles (POPC:C_{20}BAS, X_B = 0.5) on silicon (111) at room temperature. Cross sections for the lines marked on each image are shown below the images.

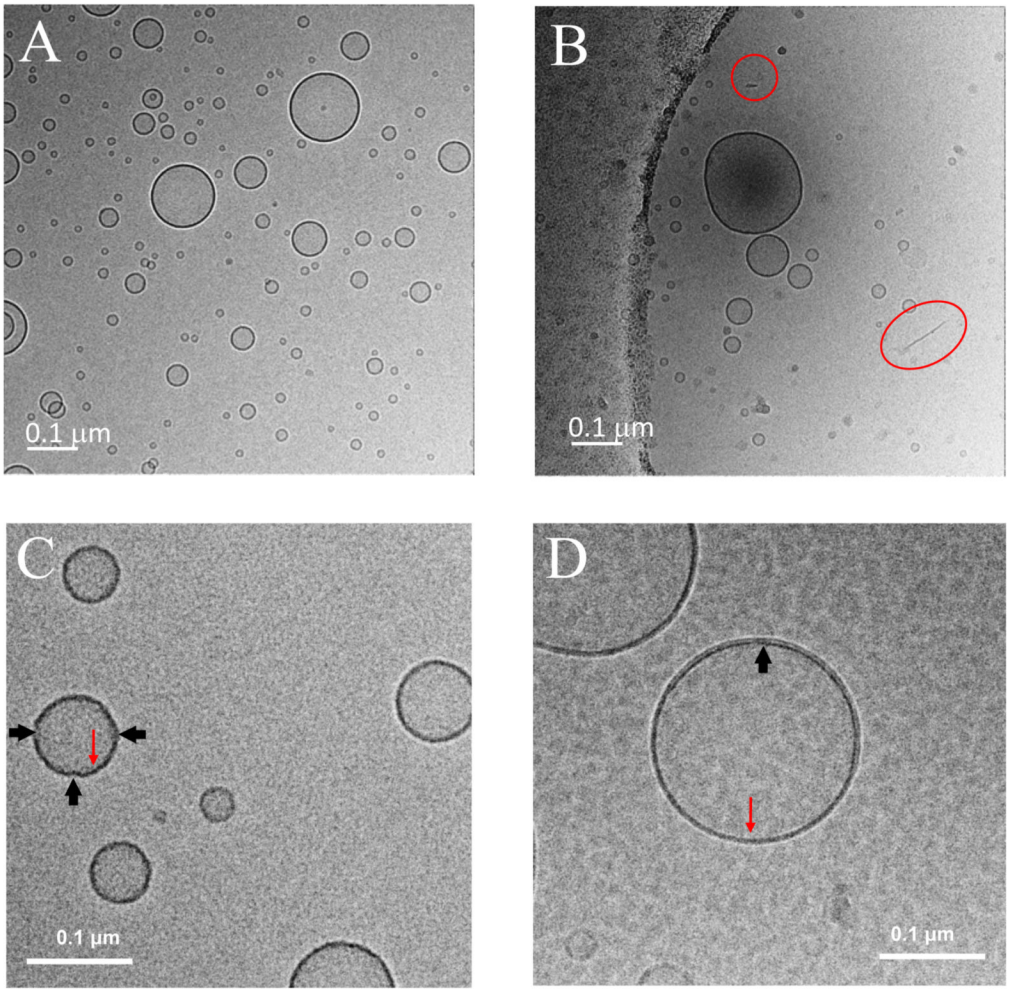

Figure 5.
CryoTEM images at 50,000× magnification of POPC:C_{20}BAS vesicles (X_B = 0.5, 30 mM total lipid) prepared by sonication (A, B) and extrusion through 200 nm filters (C, D). Image B shows one large irregularly shaped vesicle as well as several membrane fragments (outlined in red). Images C and D show vesicles where there are noticeably thicker and thinner membrane regions, indicated with thick black arrows and thin red arrows, respectively.

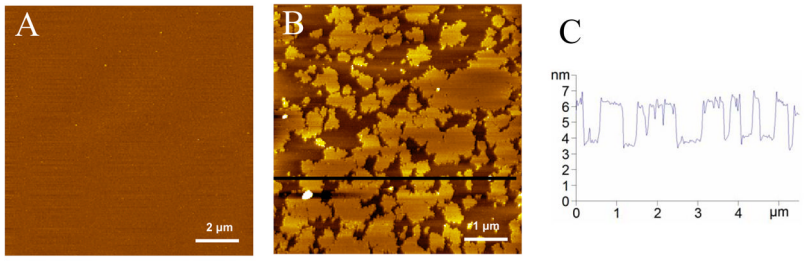

Figure 6.
AFM images for membranes prepared from extruded (A, 100 nm filter) and sonicated (B) DMPC:C_{20}BAS (X_B = 0.4) vesicles on mica. (C) Cross section for the line marked on image B.

Table 1

Mean diameters of sonicated vesicle solutions determined by dynamic light scattering.

Sample	Mean Diameter (nm)
C_{20}BAS	24
POPC	43
POPC:C_{20}BAS, X_B = 0.4	41
POPC:C_{20}BAS, X_B = 0.5	42
POPC:C_{20}BAS, X_B = 0.6	40
POPC:C_{20}BAS, X_B = 0.9	46
C_{20}BAS (after 3 days)	15
POPC (after 3 days)	39